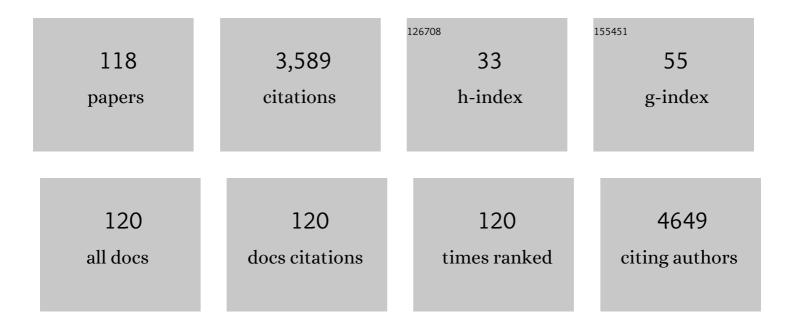
Shanming Ke

List of Publications by Year in descending order

Source: https://exaly.com/author-pdf/8714671/publications.pdf Version: 2024-02-01



#	Article	IF	CITATIONS
1	Interplay of defect dipole and flexoelectricity in linear dielectrics. Scripta Materialia, 2022, 210, 114427.	2.6	11
2	High-Temperature Flexible Transparent Heater for Rapid Thermal Annealing of Thin Films. Physical Review Applied, 2022, 17, .	1.5	1
3	The flexoelectric transition in CaCu ₃ Ti ₄ O ₁₂ material with colossal permittivity. Journal of Applied Physics, 2022, 132, 024101.	1.1	3
4	Electric Polarization Switching on an Atomically Thin Metallic Oxide. Nano Letters, 2021, 21, 144-150.	4.5	19
5	Electric modulation of conduction in MAPbBr3 single crystals. Journal of Advanced Ceramics, 2021, 10, 320-327.	8.9	11
6	Local structural heterogeneity induced large flexoelectricity in Sm-doped PMN–PT ceramics. Journal of Applied Physics, 2021, 129, .	1.1	11
7	Structural and optoelectronic properties of combining Nb-doped SrTiO3/ITO films on (0 0 1)-YSZ substrate. Results in Physics, 2021, 26, 104436.	2.0	0
8	Effects of strain on ultrahigh-performance optoelectronics and growth behavior of high-quality indium tin oxide films on yttria-stabilized zirconia (001) substrates. Journal of Materials Science: Materials in Electronics, 2021, 32, 21462-21471.	1.1	2
9	Visualization of Bubble Nucleation and Growth Confined in 2D Flakes. Small, 2021, 17, e2103301.	5.2	9
10	Visualization of Bubble Nucleation and Growth Confined in 2D Flakes (Small 39/2021). Small, 2021, 17, 2170205.	5.2	1
11	Flexible TiO2/Au thin films with greatly enhanced photocurrents for photoelectrochemical water splitting. Journal of Alloys and Compounds, 2020, 815, 152471.	2.8	13
12	Large photoelectrochemical activity of flexible TiO2/SrRuO3 oxide heterojunction. Applied Surface Science, 2020, 504, 144544.	3.1	6
13	Efficient decomplexation of heavy metal-EDTA complexes by Co2+/peroxymonosulfate process: The critical role of replacement mechanism. Chemical Engineering Journal, 2020, 392, 123639.	6.6	19
14	Atomic Steps Induce the Aligned Growth of Ice Crystals on Graphite Surfaces. Nano Letters, 2020, 20, 8112-8119.	4.5	17
15	Vibration catalysis of eco-friendly Na0.5K0.5NbO3-based piezoelectric: An efficient phase boundary catalyst. Applied Catalysis B: Environmental, 2020, 279, 119353.	10.8	128
16	Perovskite MAPb(Br1â^'Cl)3 single crystals: Solution growth and electrical properties. Journal of Crystal Growth, 2020, 549, 125869.	0.7	7
17	Epitaxial array of Fe3O4 nanodots for high rate high capacity conversion type lithium ion batteries electrode with long cycling life. Nano Energy, 2020, 74, 104876.	8.2	51
18	Nano-electrical conductivity guided optimization of pulsed laser deposited ZnO electron transporting layer for efficient perovskite solar cell. Journal of Power Sources, 2020, 468, 228392.	4.0	8

#	Article	IF	CITATIONS
19	Atomic-Scale insight into the reversibility of polar order in ultrathin epitaxial Nb:SrTiO3/BaTiO3 heterostructure and its implication to resistive switching. Acta Materialia, 2020, 188, 23-29.	3.8	12
20	Photoflexoelectric effect in halide perovskites. Nature Materials, 2020, 19, 605-609.	13.3	132
21	Ultrasonic vibration driven piezocatalytic activity of lead-free K0.5Na0.5NbO3 materials. Ceramics International, 2019, 45, 22486-22492.	2.3	59
22	Versatile and Highly Efficient Controls of Reversible Topotactic Metal–Insulator Transitions through Proton Intercalation. Advanced Functional Materials, 2019, 29, 1907072.	7.8	28
23	High-temperature ferromagnetic insulating phase in strained La0.8Sr0.2MnO3 thin films. Journal Physics D: Applied Physics, 2019, 52, 485001.	1.3	5
24	Large flexoelectric response in PMN-PT ceramics through composition design. Applied Physics Letters, 2019, 115, .	1.5	16
25	Designing electron transporting layer for efficient perovskite solar cell by deliberating over nano-electrical conductivity. Solar Energy Materials and Solar Cells, 2019, 200, 109995.	3.0	10
26	Negative Coriolis effect in piezoelectric metamaterials. Journal of Alloys and Compounds, 2019, 801, 262-266.	2.8	2
27	Flexoelectric materials and their related applications: A focused review. Journal of Advanced Ceramics, 2019, 8, 153-173.	8.9	127
28	Epitaxial ultrathin Au films on transparent mica with oxide wetting layer applied to organic light-emitting devices. Applied Physics Letters, 2019, 114, 081902.	1.5	12
29	Revisit of amorphous semiconductor InGaZnO4: A new electron transport material for perovskite solar cells. Journal of Alloys and Compounds, 2019, 789, 276-281.	2.8	16
30	A novel and sensitive sarcosine biosensor based on organic electrochemical transistor. Electrochimica Acta, 2019, 307, 100-106.	2.6	35
31	Facile fabrication of highly efficient ETL-free perovskite solar cells with 20% efficiency by defect passivation and interface engineering. Chemical Communications, 2019, 55, 2777-2780.	2.2	61
32	Pulsed laser deposition of amorphous InGaZnO ₄ as an electron transport layer for perovskite solar cells. Journal of Advanced Dielectrics, 2019, 09, 1950042.	1.5	4
33	Non-linear behavior of flexoelectricity. Applied Physics Letters, 2019, 115, .	1.5	14
34	Origin of Ferroelectricity in Epitaxial Si-Doped HfO ₂ Films. ACS Applied Materials & Interfaces, 2019, 11, 4139-4144.	4.0	48
35	A monolithically integrated photonic microwave generator. Laser Physics Letters, 2018, 15, 016201.	0.6	2
36	Black phosphorus quantum dots as dual-functional electron-selective materials for efficient plastic perovskite solar cells. Journal of Materials Chemistry A, 2018, 6, 8886-8894.	5.2	80

#	Article	IF	CITATIONS
37	High-Quality AZO/Au/AZO Sandwich Film with Ultralow Optical Loss and Resistivity for Transparent Flexible Electrodes. ACS Applied Materials & Interfaces, 2018, 10, 16160-16168.	4.0	45
38	van der Waals epitaxy of Al-doped ZnO film on mica as a flexible transparent heater with ultrafast thermal response. Applied Physics Letters, 2018, 112, .	1.5	43
39	Ferroelastic domain structure and phase transition in single-crystalline [PbZn1/3Nb2/3O3]1-x[PbTiO3]x observed via in situ x-ray microbeam. Journal of the European Ceramic Society, 2018, 38, 1488-1497.	2.8	4
40	A novel protein binding strategy for energy-transfer-based photoelectrochemical detection of enzymatic activity of botulinum neurotoxin A. Electrochemistry Communications, 2018, 97, 114-118.	2.3	5
41	Flexoelectric fatigue in (K,Na,Li)(Nb,Sb)O3 ceramics. Applied Physics Letters, 2018, 113, .	1.5	13
42	Thermal-evaporated selenium as a hole-transporting material for planar perovskite solar cells. Solar Energy Materials and Solar Cells, 2018, 185, 130-135.	3.0	22
43	Modulation of Abnormal Poisson's Ratios and Electronic Properties in Mixed-Valence Perovskite Manganite Films. ACS Applied Materials & Interfaces, 2018, 10, 18029-18035.	4.0	13
44	Ionic liquid modified SnO ₂ nanocrystals as a robust electron transporting layer for efficient planar perovskite solar cells. Journal of Materials Chemistry A, 2018, 6, 22086-22095.	5.2	66
45	Large increase of Curie temperature in (110)-oriented La0.7Sr0.3MnO3 films. Ceramics International, 2018, 44, 13695-13698.	2.3	7
46	Organic Photoâ€Electrochemical Transistorâ€Based Biosensor: A Proofâ€ofâ€Concept Study toward Highly Sensitive DNA Detection. Advanced Healthcare Materials, 2018, 7, e1800536.	3.9	54
47	Epitaxial ferroelectric Hf _{0.5} Zr _{0.5} O ₂ thin film on a buffered YSZ substrate through interface reaction. Journal of Materials Chemistry C, 2018, 6, 9224-9231.	2.7	38
48	Synthesis of ferroelectric KNbO 3 nanosheets by liquid exfoliation of layered perovskite K 2 NbO 3 F. Journal of Alloys and Compounds, 2017, 698, 357-363.	2.8	8
49	Ferroelectricâ€Enhanced Polysulfide Trapping for Lithium–Sulfur Battery Improvement. Advanced Materials, 2017, 29, 1604724.	11.1	149
50	Effect of oxygen pressure on pulsed laser deposited WO3 thin films for photoelectrochemical water splitting. Journal of Alloys and Compounds, 2017, 722, 913-919.	2.8	21
51	Performance of a building-integrated photovoltaic/thermal system under frame shadows. Energy and Buildings, 2017, 134, 71-79.	3.1	19
52	Panchromatic thin perovskite solar cells with broadband plasmonic absorption enhancement and efficient light scattering management by Au@Ag core-shell nanocuboids. Nano Energy, 2017, 41, 654-664.	8.2	68
53	Flexoelectric behavior in PIN-PMN-PT single crystals over a wide temperature range. Applied Physics Letters, 2017, 111, .	1.5	23
54	Origin of colossal dielectric response in (In + Nb) co-doped TiO2 rutile ceramics: a potential electrothermal material. Scientific Reports, 2017, 7, 10144.	1.6	18

2.1

13

#	Article	IF	CITATIONS
55	Large nonlinear dielectric behavior in BaTi1â^'xSnxO3. Scientific Reports, 2017, 7, 6693.	1.6	24
56	Interfaces between hexagonal and cubic oxides and their structure alternatives. Nature Communications, 2017, 8, 1474.	5.8	31
57	A sensitive DNA sensor based on an organic electrochemical transistor using a peptide nucleic acid-modified nanoporous gold gate electrode. RSC Advances, 2017, 7, 52118-52124.	1.7	27
58	A Novel Organic Electrochemical Transistor-Based Platform for Monitoring the Senescent Green Vegetative Phase of Haematococcus pluvialis Cells. Sensors, 2017, 17, 1997.	2.1	11
59	1-Butyl-3-Methylimidazolium Tetrafluoroborate Film as a Highly Selective Sensing Material for Non-Invasive Detection of Acetone Using a Quartz Crystal Microbalance. Sensors, 2017, 17, 194.	2.1	15
60	A Diagram of the Structure Evolution of Pb(Zn1/3Nb2/3) O3-9%PbTiO3 Relaxor Ferroelectric Crystals with Excellent Piezoelectric Properties. Crystals, 2017, 7, 130.	1.0	6
61	A Rapid, Label-free and Impedimetric DNA Sensor Based on PNA-modified Nanoporous Gold Electrode. International Journal of Electrochemical Science, 2017, 12, 10511-10523.	0.5	6
62	Intrinsic and extrinsic effects on the ferroelectric switching of thin poly(vinylidene) Tj ETQq0 0 0 rgBT /Overlock 10)	$2 \operatorname{Td}_{13}$ (fluorid
63	Realizing 60 GHz narrow-linewidth photonic microwaves with very low RF driving power. Laser Physics Letters, 2016, 13, 126202.	0.6	3
64	Use of a novel layered titanoniobate as an anode material for long cycle life sodium ion batteries. RSC Advances, 2016, 6, 35746-35750.	1.7	27
65	A giant negative electrocaloric effect in Eu-doped PbZrO ₃ thin films. Journal of Materials Chemistry C, 2016, 4, 3375-3378.	2.7	62
66	Morphotropic domain structures and dielectric relaxation in piezo-/ferroelectric Pb(In1/2Nb1/2)O3–Pb(Zn1/3Nb2/3)O3–PbTiO3 single crystals. Journal of Crystal Growth, 2016, 441, 33-40.	0.7	4
67	Transparent Indium Tin Oxide Electrodes on Muscovite Mica for High-Temperature-Processed Flexible Optoelectronic Devices. ACS Applied Materials & Interfaces, 2016, 8, 28406-28411.	4.0	83

68	Multichannel quartz crystal microbalance array: Fabrication, evaluation, application in biomarker detection. Analytical Biochemistry, 2016, 494, 85-92.	1.1	23
69	Structural and optical characteristics of the hexagonal ZnO films grown on cubic MgO (001) substrates. Optics Letters, 2016, 41, 4895.	1.7	5
70	Preparation and characterization of hydroxyapatite-polylactic acid HA-PLA composite film. Shenzhen Daxue Xuebao (Ligong Ban)/Journal of Shenzhen University Science and Engineering, 2016, 33, 10.	0.1	1
71	Temperature-dependent reversible and irreversible processes in Nb-doped PbZrO3 relaxor ferroelectric thin films. Applied Physics Letters, 2015, 107, .	1.5	8

⁷² Integration of a Miniature Quartz Crystal Microbalance with a Microfluidic Chip for Amyloid Beta-Al²42 Quantitation. Sensors, 2015, 15, 25746-25760.

5

#	Article	IF	CITATIONS
73	Ferroelectric Polymer Thin Films for Organic Electronics. Journal of Nanomaterials, 2015, 2015, 1-14.	1.5	35
74	Large Energy Storage Density and High Thermal Stability in a Highly Textured (111)-Oriented Pb _{0.8} Ba _{0.2} ZrO ₃ Relaxor Thin Film with the Coexistence of Antiferroelectric and Ferroelectric Phases. ACS Applied Materials & Interfaces, 2015, 7, 13512-13517.	4.0	185
75	Growth and properties of (1â^'x)Pb(Zn1/3Nb2/3)O3–xPbTiO3 (x=0.07–0.11) ferroelectric single crystals by a top-seeded solution growth method. Ceramics International, 2015, 41, 14427-14434.	2.3	9
76	High dielectric tunability, electrostriction strain and electrocaloric strength at a tricritical point of tetragonal, rhombohedral and pseudocubic phases. Journal of Alloys and Compounds, 2015, 646, 597-602.	2.8	23
77	Large electrocaloric strength in the (100)-oriented relaxor ferroelectric Pb[(Ni1/3Nb2/3)0.6Ti0.4]O3 single crystal at near morphotropic phase boundary. Ceramics International, 2015, 41, 9344-9349.	2.3	23
78	Giant Electric Energy Density in Epitaxial Leadâ€Free Thin Films with Coexistence of Ferroelectrics and Antiferroelectrics. Advanced Electronic Materials, 2015, 1, 1500052.	2.6	195
79	Structure, corrosion resistance and in vitro bioactivity of Ca and P containing TiO 2 coating fabricated on NiTi alloy by plasma electrolytic oxidation. Applied Surface Science, 2015, 356, 1234-1243.	3.1	36
80	Tuning of dielectric and ferroelectric properties in single phase BiFeO3 ceramics with controlled Fe2+/Fe3+ ratio. Ceramics International, 2014, 40, 5263-5268.	2.3	36
81	Giant dielectric response and enhanced thermal stability of multiferroic BiFeO3. Journal of Alloys and Compounds, 2014, 600, 118-124.	2.8	21
82	Glucose sensors based on solution-gated graphene transistors. Shenzhen Daxue Xuebao (Ligong) Tj ETQq0 0 0 rş	gBT /Over 0.1	ock 10 Tf 50
83	Study on dielectric properties of hyperbranched zinc phthalocyanine. Shenzhen Daxue Xuebao (Ligong) Tj ETQq1	10,7843	314 rgBT /Ovi
84	Variable-range-hopping conductivity in high-k Ba(Fe0.5Nb0.5)O3 ceramics. Journal of Applied Physics, 2013, 114, .	1.1	30
85	Mean-Field Approach to Dielectric Relaxation in Giant Dielectric Constant Perovskite Ceramics. Journal of Ceramics, 2013, 2013, 1-7.	0.9	8
86	Antiferroelectric-like properties and enhanced polarization of Cu-doped K _{0.5} Na _{0.5} NbO ₃ piezoelectric ceramics. Applied Physics Letters, 2012, 101, 082901.	1.5	71
87	Dielectric property of all-organic composite film composed of cobalt phthalocyanine and poly(vinylidene fluoride). , 2012, , .		0
88	Electrical and Dielectric Properties of Exfoliated Graphite/Polyimide Composite Films with Low Percolation Threshold. Journal of Electronic Materials, 2012, 41, 2439-2446.	1.0	14
89	Structural dependence of piezoelectric, dielectric and ferroelectric properties of K0.5Na0.5(Nb1â~2/5Cu)O3 lead-free ceramics with high Q. Materials Research Bulletin, 2012, 47, 4472-4477.	2.7	35
90	Dielectric spectroscopy of biodegradable poly(3-hydroxybutyrate-co-3-hydroxyhexanoate) films. European Polymer Journal, 2012, 48, 79-85.	2.6	15

#	Article	IF	CITATIONS
91	Dielectric and Thermal Properties of Polyimide–Poly(ethylene oxide) Nanofoamed Films. Journal of Electronic Materials, 2012, 41, 2281-2285.	1.0	12
92	Dielectric behaviors of PHBHHx–BaTiO3 multifunctional composite films. Composites Science and Technology, 2012, 72, 370-375.	3.8	10
93	Electrical modulus analysis on the Ni/CCTO/PVDF system near the percolation threshold. Journal Physics D: Applied Physics, 2011, 44, 475305.	1.3	53
94	TiO2/SiO2 hybrid nanomaterials: synthesis and variable UV-blocking properties. Journal of Sol-Gel Science and Technology, 2011, 58, 326-329.	1.1	43
95	Dielectric relaxations of high- <i>k</i> poly(butylene succinate) based all-organic nanocomposite films for capacitor applications. Journal of Materials Research, 2011, 26, 2493-2502.	1.2	14
96	Giant low frequency dielectric tunability in high-k Ba(Fe1/2Nb1/2)O3 ceramics at room temperature. Journal of Applied Physics, 2010, 108, 064104.	1.1	23
97	Revisit of the Vögel–Fulcher freezing in lead magnesium niobate relaxors. Applied Physics Letters, 2010, 97, 132905.	1.5	30
98	Crossover from a nearly constant loss to a superlinear power-law behavior in Mn-doped Bi(Mg1/2Ti1/2)O3–PbTiO3 ferroelectrics. Journal of Applied Physics, 2010, 107, .	1.1	29
99	Dielectric relaxation in A2FeNbO6 (A = Ba, Sr, and Ca) perovskite ceramics. Journal of Electroceramics, 2009, 22, 252-256.	0.8	75
100	Relaxor behavior and electrical properties of high dielectric constant materials. Science in China Series D: Earth Sciences, 2009, 52, 2180-2185.	0.9	11
101	Nearly constant dielectric loss behavior in poly(3-hydroxybutyrate- <i>co</i> -3-hydroxyvalerate) biodegradable polyester. Journal of Applied Physics, 2009, 105, .	1.1	37
102	Relaxor behavior and dielectric properties of lead magnesium niobate–lead titanate thick films prepared by electrophoresis deposition. Journal of Alloys and Compounds, 2009, 478, 853-857.	2.8	19
103	Structure and properties of PMN–PT/NZFO laminates and composites. Ceramics International, 2008, 34, 701-704.	2.3	8
104	Colossal dielectric response in barium iron niobate ceramics obtained by different precursors. Ceramics International, 2008, 34, 1059-1062.	2.3	53
105	Low-temperature growth of lead magnesium niobate thick films by a hydrothermal process. Ceramics International, 2008, 34, 1063-1066.	2.3	6
106	Structural and electric properties of barium strontium titanate based ceramic composite as a humidity sensor. Solid State Ionics, 2008, 179, 1632-1635.	1.3	24
107	Effect of sintering temperature on the structure and properties of cerium-doped 0.94(Bi0.5Na0.5)TiO3–0.06BaTiO3 piezoelectric ceramics. Journal of Alloys and Compounds, 2008, 458, 504-508.	2.8	78
108	MgTiO3 doping effect on dielectric properties of Ba0.6Sr0.4TiO3 ceramics via a molten salt process. Composites Part A: Applied Science and Manufacturing, 2008, 39, 597-601.	3.8	12

#	Article	IF	CITATIONS
109	Lorentz-type relationship of the temperature dependent dielectric permittivity in ferroelectrics with diffuse phase transition. Applied Physics Letters, 2008, 93, .	1.5	85
110	Dielectric, ferroelectric properties, and grain growth of CaxBa1â^'xNb2O6 ceramics with tungsten-bronzes structure. Journal of Applied Physics, 2008, 104, .	1.1	37
111	Dielectric relaxation in polyimide nanofoamed films with low dielectric constant. Applied Physics Letters, 2008, 92, .	1.5	25
112	Dielectric dispersion behavior of Ba(ZrxTi1â^'x)O3 solid solutions with a quasiferroelectric state. Journal of Applied Physics, 2008, 104, .	1.1	56
113	Dielectric and ageing behaviour of strontium barium niobate with barium strontium titanate additives. Journal Physics D: Applied Physics, 2007, 40, 6797-6802.	1.3	7
114	Micro-Raman scattering and DC field dependent dielectric properties of BaZr x Ti 1 - x O 3 relaxor ferroelectric ceramics. Proceedings of SPIE, 2007, , .	0.8	2
115	Slow relaxation of piezoelectric response in CdZnTe ferroelectric semiconductor single crystals. Applied Physics Letters, 2007, 91, .	1.5	4
116	Microstructure evolutions and electrical properties of Pb1â^'xLax(Zr0.56Ti0.44)1â^'x/4O3 ceramics. Materials Science and Engineering B: Solid-State Materials for Advanced Technology, 2007, 138, 205-209.	1.7	8
117	Relaxor behavior in CaCu3Ti4O12 ceramics. Applied Physics Letters, 2006, 89, 182904.	1.5	128
118	Low-temperature synthesis of (Pb,La)(Zr,Ti)O3 thick film on Ti substrates by the hydrothermal method using oxide precursors. Applied Physics Letters, 2006, 88, 012901.	1.5	6